Quantum Chemical Studies on Structures and Spectra of 2,5-Distyrylpyrazine (DSP) Laser Dye

AHMED M. EL-NAHAS,[1] ESSAM HAMMAM,[2] EL-ZEINY M. EBEID[3]

[1] *Chemistry Department, Faculty of Science, El-Menoufia University, Shebin El-Kom, Egypt*
[2] *Chemistry Department, Faculty of Science, Tanta University, Tanta, Egypt*
[3] *Misr University for Science and Technology (MUST), 6th October City, Egypt*

Received 10 June 1997; accepted 22 October 1997

ABSTRACT: Semiempirical (MNDO and PM3) molecular orbital calculations have been undertaken to study the structures of the ground and excited states of 2,5-distrylpyrazine dye to assess its activity as a laser dye. In the ground and first excited singlet states, the trans-trans structure of C_{2h} symmetry is the most stable structure in the gas phase and in DMSO, which agrees with the experimental findings. Upon excitation, the flexibility of the molecule decreases, leading to a subsequent decrease in the radiationless deactivation pathway and this increases the fluorescence efficiency of DSP. The absorption, excitation, and emission spectra have been calculated at the MNDO level using the PM3 optimized geometries in DMSO. At this level the agreement between theory and experiment is quite good. An estimated absorption band at 377 nm (expt 380 nm) is assigned to the $S_0 \rightarrow S_1$ transition. The excited state absorption band at 457 nm (expt 460 nm) is assigned to the $S_1 \rightarrow S_{12}$ transition. The emission band at 458 nm (expt 460 nm) is assigned to the $S'_1 \rightarrow S'_0$ transition. The overlap between the emission and the excited-state absorption spectra is presumably the main reason behind the reduced laser activity of the investigated dye. J Comput Chem 19: 585–592, 1998

Keywords: semiempirical calculations; electronic spectra; conformational analysis; 2,5-distyrylpyrazine laser dye

Correspondence to: A. M. El-Nahas; e-mail: science@shebin.eun.eg

CCC 0192-8651 / 98 / 060585-08

Introduction

Several diolefinic dyes are well known blue emitting laser dyes.[1–4] These include the styryl benzene derivatives and their nitrogen heterocyclic analogs of the general formula

$$\text{Ar—CH=CH—Ar'—CH=CH—Ar},$$

where Ar and Ar′ are aromatic moieties and either Ar or Ar′ contains nitrogen heteroatom(s).

Several criteria have been reported for these dyes. These include molecular association in the ground[5] and excited[6,7] states, excited-state absorption (ESA),[8] solubility limitations,[8] and acid–base properties.[3] In the present series of laser dyes it was realized that dyes containing pyrazinyl moieties are generally less efficient dyes compared with those containing the pyridyl ones.[9] The tendency to molecular aggregation also increases in pyrazinyl derivatives compared with pyridyl ones.[9] The position of ESA maxima relative to the laser emission maxima obviously plays an important role in that respect. Other factors include triplet state generation, molecular aggregation, photostability, etc. 2,5-Distyrylpyrazine (DSP) is one of the earliest reported compounds in this series.[10] In solution,[11] DSP belongs to the C_{2h} point group and in the solid state[12] it has C_1 symmetry. According to symmetry rules in the C_{2h} point group, the only allowed π, π^* transitions are those to electronic states of B_u symmetry. Thus, the S_1 electronic state of DSP is of this character.[11] Assignment of the electronic excitations in this molecule is of considerable importance in interpreting the results of photochemical experiments. Computational studies on the excited state absorption of the types ($S_1 \rightarrow S_n$) and ($T_1 \rightarrow T_n$) were performed earlier for polyene dyestuffs,[13] but theoretical investigations on DSP are not available. Semiempirical MNDO,[14] AM1,[15] and PM3[16] methods were concerned mainly with calculations on ground and low-lying excited states of organic molecules. In this research we attempted to study ground (S_0) and excited states (S_n and T_n) of DSP laser dye as a member of the present diolefinic series using PM3 and MNDO Hamiltonians in DMSO in an attempt to correlate the computational data with the available experimental results.

Methodology

All calculations were performed with the VAMP program,[17] which is input-compatible with MOPAC[18] and AMPAC.[19] The geometries of different conformations of DSP dye were fully optimized using the PM3 Hamiltonian in the gas phase as well as in DMSO solvent. The PRECISE option was implemented, as recommended,[20] for augmenting the convergence criteria for the consistent field iterations and for geometry optimization. The solvent effect was introduced through the self-consistent reaction field (SCRF) model.[21] All geometries were fully optimized at C_1 symmetry (i.e., no symmetry constraint). For calculation of electronic spectra we used configuration interaction (CI) expansion limiting the CI to single and pair double excitations (PECI = 10). The SCRF model along with this CI expansion gave reliable spectra for organic dyes.[21] The ROOT, SINGLET, TRIPLET, and OPEN options were also used to assign electrons to definite states.[17] The electronic excitations are vertical in nature.[22] Absorption ($S_0 \rightarrow S_1$), excitation ($S_1 \rightarrow S_n$, $T_1 \rightarrow T_n$) and emission ($S_1' \rightarrow S_0'$) spectra were calculated at the MNDO level using the PM3 optimized geometries in DMSO. All the excited states were calculated at the restricted open-shell Hartree–Fock (ROHF) level. As far as the absorption spectra is concerned, a good agreement between the experimental[9] and theoretical $\lambda_{abs.}$ is obtained if S_0 and S_1 states are calculated at restricted Hartree–Fock (RHF) level. Ionization potentials were calculated using Koopmans' theorem,[23] which states that for closed-shell systems, the ionization potential is the negative of the corresponding molecular orbital eigenvalue.

The potential energy surface describing internal rotation around the single bond linking the pyrazine moiety with the ethylenic double bond for DSP is obtained by allowing the torsional dihedral angle C7C8C9N11 (Fig. 1) to vary by 10° increments while optimizing all other structural parameters. The conformational analysis was done through the Fourier expansion[24] $V(\phi)$, which is

$$V((\phi)) = \tfrac{1}{2}\sum_n Vn(1 + \cos n\phi) + \tfrac{1}{2}\sum_n V'n(1 + \sin n\phi),$$

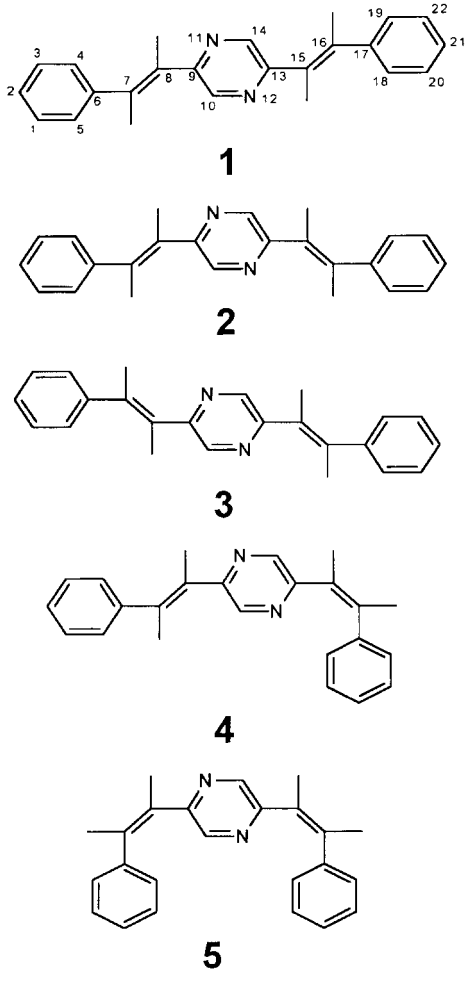

FIGURE 1. PM3 optimized structures for 2,5-distyrylpyrazine (DSP) in DMSO.

where ϕ is the angle of rotation. Frequently, the expansion is symmetric around $\phi = 0$, so the sine terms disappear. In addition, the series is generally truncated after three terms. The most commonly used form of expansion is then

$$V(\phi) = \tfrac{1}{2}\sum_n Vn(1 + \cos n\phi)$$
$$= \tfrac{1}{2}V_1(1 + \cos\phi) + \tfrac{1}{2}V_2(1 + \cos 2\phi) + \tfrac{1}{2}V_3(1 + \cos 3\phi)$$
$$= V_1(\phi) + V_2(\phi) + V_3(\phi),$$

where

$$V_1(\phi) = \tfrac{1}{2}V_1(1 + \cos\phi),$$
$$V_2(\phi) = \tfrac{1}{2}V_2(1 + \cos 2\phi),$$
$$V_3(\phi) = \tfrac{1}{2}V_3(1 + \cos 3\phi).$$

The individual components $V_1(\phi)$, $V_2(\phi)$, and $V_3(\phi)$ can be identified with specific physical effects because of their periodic properties. $V_1(\phi)$ corresponds to dipolar or steric interactions, $V_2(\phi)$ corresponds to conjugative or hyperconjugative interactions, and $V_3(\phi)$ corresponds to repulsion between bonding pairs of electrons.

Results and Discussion

The calculated heats of formation of different structures in the states S_0, S_1, and T_1 are given in Table I. Dipole moments and ionization potentials for the investigated species are listed in Table II. A comparison between X-ray data with optimized geometries calculated at PM3 in DMSO is shown in Table III, whereas between ground and excited singlet and triplet states is listed in Table IV. The calculated bond orders and charge distributions are presented in Table V. Figure 1 shows the optimized structures for DSP at the PM3 level in DMSO. Calculated potential function, $V(\phi)$, and the Fourier components, $V_n(\phi)$, for DSP are displayed in Figures 2 and 3. The energies of different electronic states are depicted in Figure 4.

Some of the earlier work on conformational analysis has shown that, as one proceeds from the gaseous to the condensed phases, the conformations having the higher dipole moment frequently become stabilized more in the liquid because of intermolecular dipole–dipole interaction.[25] The large difference in ΔH_f and in conformation in going from the gas to the liquid indicates a strong intermolecular association in the liquid phase. An inspection of Table II reveals that in the ground state, the dipole moment is small and therefore ΔH_f does not change significantly when going from the gaseous to the liquid phase. On the other hand, in the first excited singlet and triplet states the dipole moments are large and the stabilization in the solvent (DMSO) is pronounced, and this is reflected in large differences in ΔH_f in the two phases (Table I).

An insight into Figure 2 indicates that DSP exists mainly as two equivalent structures **1** and **2** in the liquid state (Fig. 1). The energy barrier between these two forms is estimated to be ~ 2 kcal/mol. In both conformers, the phenyl rings are in trans orientation with respect to the pyrazine moiety. The low rotational barrier may indicate that these two conformers are interconvertable at

TABLE I.
Heats of Formation (kcal / mol) for DSP in Gas and Liquid Phases at PM3.

	Gas phase			DMSO		
Structure	S_0	S_1	T_1	S_0	S_1	T_1
trans-trans	114.99	235.67	159.36	114.91	210.46	160.53
cis-trans	118.85	243.96	160.23	118.80	210.46	166.90
cis-cis	125.29	228.92	166.86	122.59	216.11	183.15

TABLE II.
Dipole Moments (DM) and Ionization Potentials (IP) Calculated at PM3 for DSP in Gas Phase.

	DM (D)			IP (eV)		
Structure	S_0	S_1	T_1	S_0	S_1	T_1
trans-trans	0.001	2.677	0.056	8.655	4.508	4.011
cis-trans	0.334	2.457	1.345	8.830	4.552	4.029
cis-cis	0.444	1.756	1.488	9.006	4.139	3.979

D, debyes.

room temperature. A third isoenergetic conformer **3** was calculated where the two ethylenic double bonds are syn with respect to the nitrogen atoms. We call these three forms trans-trans structures. Another two structures can be located on the potential energy surface of the DSP molecule. In the first, one of the phenyl rings is in a cis position with respect to the pyrazine center. This one is called cis-trans form **4**. In the second case, both of the phenyl rings are in cis orientation with respect to the pyrazine moiety and this is referred to as cis-cis isomer **5**. The trans-trans form is more stable than the other two structures (Table I); the cis-cis isomer is the least stable species. The trans-trans form has a negligible dipole moment due to its high symmetry (C_{2h}) and, therefore, a negligible solvent stabilization. The cis-trans and cis-cis conformers have even smaller dipole moments and the stabilization in the solvent is not clear. The cis-trans and cis-cis forms can both be obtained photochemically upon UV irradiation in dilute solutions as reported earlier.[26]

TABLE III.
Optimized Geometries for DSP at PM3 in DMSO Compared with X-Ray Data.

Bond lengths (Å)	PM3	X ray	Bond angles (°)	PM3	X ray
C1–C2	1.392	1.394	C1C2C3	119.96	119.4
C1–C5	1.389	1.389	C2C1C5	120.25	120.1
C2–C3	1.391	1.394	C2C3C4	120.04	120.6
C3–C4	1.389	1.389	C3C4C6	120.33	120.7
C4–C6	1.399	1.412	C4C6C7	120.98	119.6
C5–C6	1.399	1.405	C4C6C5	119.35	117.7
C6–C7	1.457	1.469	C6C5C1	120.07	121.5
C7–C8	1.343	1.330	C6C7C8	122.89	127.0
C8–C9	1.457	1.463	C7C8C9	121.34	126.0
C9–C10	1.409	1.395	C8C9C10	122.26	120.8
C9–N11	1.365	1.364	C8C9N11	118.09	119.0
C10–N12	1.347	1.328	C9C10N12	121.34	124.1
			C9N11C14	118.91	115.8

TABLE IV.
Optimized Geometries for DSP at PM3 in DMSO in Different Electronic States.

Bond lengths (Å)	S_0	S_1	T_1	Bond lengths (Å)	S_0	S_1	T_1
C1–C2	1.392	1.395	1.396	N12–C13	1.365	1.415	1.409
C1–C5	1.389	1.384	1.385	N11–C14	1.347	1.309	1.308
C9–C3	1.391	1.395	1.396	C13–C14	1.409	1.453	1.450
C3–C4	1.389	1.383	1.384	C13–C15	1.457	1.387	1.387
C4–C6	1.399	1.412	1.413	C15–C16	1.343	1.395	1.395
C5–C6	1.399	1.413	1.414	C16–C17	1.457	1.419	1.419
C6–C7	1.457	1.419	1.419	C17–C18	1.399	1.412	1.413
C7–C8	1.343	1.395	1.395	C17–C19	1.399	1.413	1.414
C8–C9	1.457	1.387	1.387	C18–C20	1.389	1.383	1.384
C9–C10	1.409	1.453	1.450	C19–C22	1.389	1.384	1.385
C9–N11	1.365	1.415	1.409	C20–C21	1.391	1.395	1.396
C10–N12	1.347	1.309	1.308	C21–C22	1.392	1.395	1.396
Bond angles (°)				Bond angles (°)			
C1C2C3	119.96	119.89	119.77	N11C14C13	121.34	122.63	121.68
C2C1C5	120.25	120.43	120.51	N12C13C14	119.75	118.19	118.66
C2C3C4	120.04	120.26	120.36	C14C13C15	122.16	123.08	123.39
C3C4C6	120.33	120.56	120.53	N12C13C15	118.09	118.73	117.95
C4C6C7	120.98	121.59	121.57	C13C15C16	122.04	122.49	121.71
C4C6C5	119.35	118.53	118.51	C15C16C17	122.89	122.93	123.32
C6C5C1	120.07	120.33	120.33	C16C17C18	120.98	121.59	121.55
C6C7C8	122.89	122.93	123.36	C16C17C19	119.67	119.88	119.95
C7C8C9	121.34	122.49	121.67	C17C18C20	120.33	120.56	120.56
C8C9C10	122.26	123.08	123.37	C17C19C22	120.07	120.33	120.32
C8C9N11	118.09	118.73	117.98	C18C20C21	120.04	120.26	120.33
C9C10N12	121.34	122.63	121.68	C19C22C21	120.25	120.43	120.52
C9N11C14	118.91	119.18	119.66	C20C21C22	119.96	119.89	119.77

TABLE V.
Bond Orders and Charge Distributions for DSP at PM3 in DMSO in Different Electronic States.

	Bond orders				Charge distributions		
Connected atoms	S_0	S_1	T_1	Atom center	S_0	S_1	T_1
C1–C2	1.417	1.389	1.398	C1	−0.104	−0.104	−0.105
C1–C5	1.437	1.476	1.466	C2	−0.093	−0.085	−0.089
C2–C3	1.419	1.388	1.397	C3	−0.100	−0.100	−0.101
C3–C4	1.434	1.476	1.466	C4	−0.092	−0.092	−0.093
C4–C6	1.381	1.288	1.315	C5	−0.085	−0.085	−0.087
C5–C6	1.379	1.288	1.315	C6	−0.058	−0.042	−0.047
C6–C7	1.042	1.213	1.169	C7	−0.073	−0.100	−0.095
C7–C8	1.839	1.364	1.519	C8	−0.105	−0.048	−0.064
C8–C9	1.037	1.427	1.304	C9	−0.054	−0.121	−0.095
C9–C10	1.335	1.066	1.154	C10	−0.106	−0.060	−0.072
C9–N11	1.384	1.103	1.190	N11	−0.029	−0.053	−0.043
C10–N12	1.470	1.759	1.673	N12	−0.029	−0.053	−0.043
N12–C13	1.384	1.103	1.190	C13	−0.054	−0.121	−0.095
N11–C14	1.470	1.759	1.673	C14	−0.106	−0.060	−0.072
C13–C14	1.335	1.066	1.155				

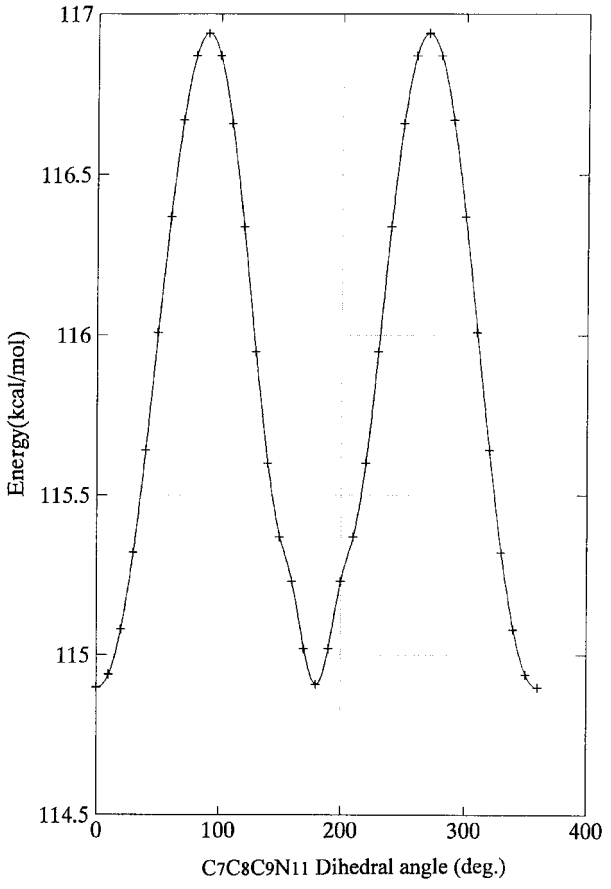

FIGURE 2. Potential function $V(\varphi)$ describing internal rotation in DSP in DMSO.

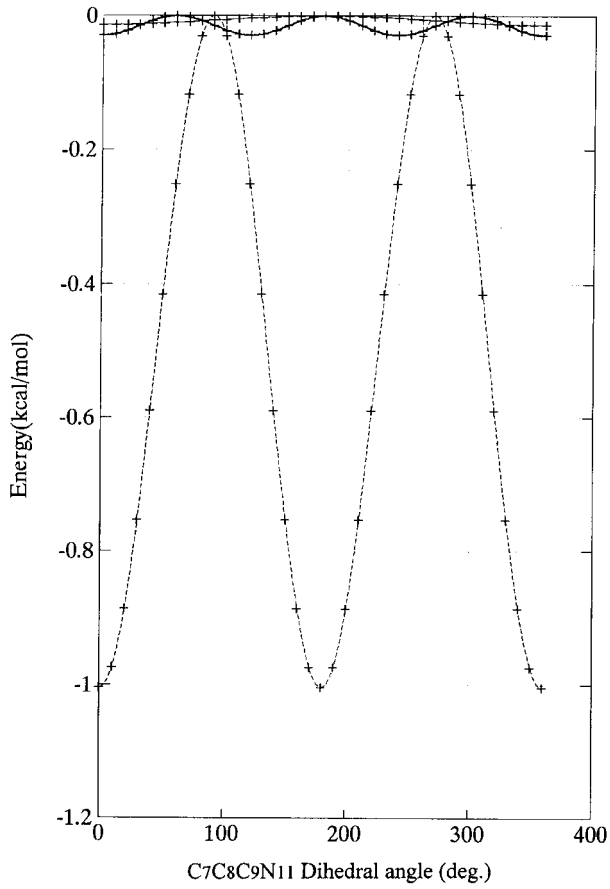

FIGURE 3. Fourier components (—) $V_1(\varphi)$, (- - -) $V_2(\varphi)$, and (···) $V_3(\varphi)$ of the potential function $V(\varphi)$ describing internal rotation in DSP in DMSO.

The large singlet–triplet splitting energies $\Delta E_{S,T}$ are consistent with π, π^* electronic states because n, π^* states are usually associated with low $\Delta E_{S,T}$ values.[27] A low $\Delta E_{S,T}$ value would favor $S_n \rightarrow T_n$ intersystem crossing. The population of excited triplet states plays an important role in suppressing laser action. It is clear from the data in Table I that $\Delta E_{S,T}$ for the trans-trans structure is of the order of ca. 50 kcal/mol in DMSO, which is consistent with a π, π^* state as reported earlier.[11] In both the gas and liquid phases, the S_1 state is optimized to C_{2h} structure. This is in accord with the experimental[11] foundation that indicates that according to symmetry rules in the C_{2h} point group, the only allowed π, π^* transitions are those to electronic states of B_u symmetry.

The PM3 method normally reproduces ground-state geometries accurately.[28] The average errors in bond lengths are 0.036 Å, for angles are 3.9°, and for dihedrals, of which insufficient data were used to assure the statistical significance of the results, 14.9°. Table III reveals a good agreement between the X-ray geometry[12] and that calculated at the PM3 level in DMSO. This substantiates the reliability of the PM3 model to give correct structures for such laser dyes. Table IV shows that upon excitation bond lengths change and some bonds become longer and others become shorter. This means that most bonds have a partial π-bond character in the excited states. The bond order of C7–C8 decreases, while those of C6–C7 and C8–C9 increase upon electronic excitation (Table V). This suppresses the free rotation of terminal phenyl rings with a subsequent decrease in efficiency of the radiationless deactivation pathway, and this increases the fluorescence efficiency[10] of these molecules and plays an important role in laser action.

In the ground state, and due to localization of a lone pair of electrons on the nitrogen atoms in the pyrazinyl moiety, the pyrazine moiety is more rich in electron cloud compared with the phenyl moieties (Table V). An interaction between the elec-

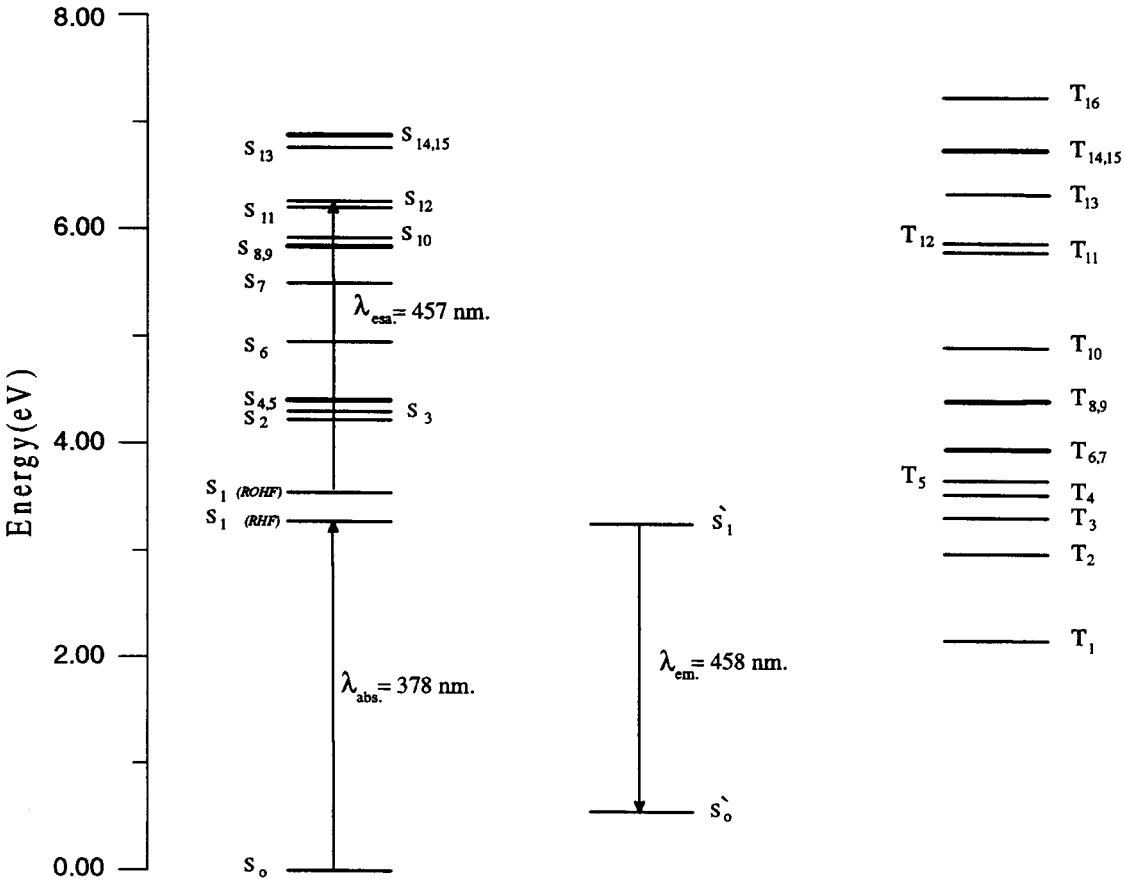

FIGURE 4. Energy level diagram of the calculated singlet and triplet states of the trans-trans structure of DSP in DMSO. Vertical arrows indicate the corresponding measured[9] λ_{max}. S_1 (RHF) and S_1 (ROHF) represent the first excited singlet states calculated using restricted Hartree–Fock and restricted open-shell Hartree–Fock levels, respectively.

tron-rich pyrazine moiety and the relatively electron-deficient phenyl moieties leads to a stacklike structure in which molecules are half-shifted with respect to each other. Such stacking has been observed for room temperature α-DSP crystals.[29] The similarity between solution and solid-state structures may explain the agreement between solution calculated geometries and X-ray geometries. Upon electronic excitation to S_1, electron charges are redistributed and the electron densities on the heteronitrogen atoms increase (Table V). This implies more the basic character of the excited state compared with the ground state. A similar behavior was observed experimentally for the quinolyl diolefinic analog.[3]

The rotational potential constants V_1, V_2, and V_3 are all negative at -0.0134, -1.0039, and -0.0289 kcal/mol, respectively. V_1 and V_3 are very small and the potential function is dominated by a large negative V_2 term, leading to equivalent minima at the cis and trans conformations at the expense of orthogonal structures (Fig. 3). At these configurations the conjugative interaction is maximum. The overall result is a potential curve with equivalent minima at the cis and trans positions. These findings are consistent with the results obtained experimentally in solution[11] and in the solid state,[12] which indicates that the trans-trans form is the most stable structure for DSP in the ground state.

The different electronic transitions displayed in Figure 4 agree well with the available experimental data.[9] The absorption ($S_0 \rightarrow S_1$), excitation ($S_1 \rightarrow S_n$, $T_1 \rightarrow T_n$), and emission ($S'_1 \rightarrow S'_0$) spectra were calculated at the MNDO level using the PM3 optimized geometries in DMSO. The estimated absorption band is at 377 nm (expt 380 nm) and is assigned to the $S_0 \rightarrow S_1$ transition. A strong ESA band occurs at 457 nm (expt 460 nm) and is assigned to the $S_1 \rightarrow S_{12}$ transition. An emission band at 458 nm (expt 460 nm) is assigned to the $S'_1 \rightarrow S'_0$ transition. The overlap between the emission spectrum with that of the ESA is probably the main

reason behind the reduced laser activity of the investigated dye.

References

1. S. Yongjia and R. Shengwa, *Dyes Pigments*, **15**, 157 (1991) and references therein.
2. S. A. El-Daly, S. M. Al-Hazmy, E. M. Ebeid, and E. M. Vernigor, *J. Photochem. Photobiol. A: Chem.*, **91**, 199 (1995).
3. S. A. El-Daly, S. M. Al-Hazmy, E. M. Ebeid, A. C. Bhasikuttan, D. K. Palit, A. V. Spare, and J. P. Mittal, *J. Phys. Chem.*, **100**, 9732 (1996) and references therein.
4. O. Uchino, T. Mizunami, M. Maeda, and Y. Miyazoe, *Appl. Phys.*, **19**, 35 (1979).
5. E. M. Ebeid, R. M. Issa, M. M. Ghonein, and S. A. El-Daly, *J. Chem. Soc. Faraday Trans. 1*, **82**, 909 (1986).
6. F. Suzuki, T. Tamaki, and M. Hasegawa, *Bull. Chem. Soc. Jpn.*, **82**, 210 (1974).
7. E. M. Ebeid and A. J. Lees, *J. Phys. Chem.*, **91**, 5792 (1987).
8. S. A. El-Daly, E. M. Ebeid, S. M. Al-Hazmy, A. S. Babaqi, Z. El-Gohary, and G. Duportail, *Proc. Ind. Acad. Sci.* (*Chem. Sci.*), **105**, 651 (1993).
9. E. M. Ebeid, S. A. El-Daly, S. M. Al-Hazmy, and E. Dallrozzo, unpublished results.
10. E. M. Ebeid, M. M. F. Sabry, and S. A. El-Daly, *Laser Chem.*, **5**, 223 (1985).
11. J. O. Williams and K.-J. Styrcz, *Chem. Phys. Lett.*, **69**, 83 (1980).
12. Y. Sasada, H. Shimanouchi, H. Nakanishi, and M. Hasegawa, *Bull. Chem. Soc. Jpn.*, **44**, 1262 (1971).
13. M. Sadrai, L. Hadel, R. R. Sauers, S. Husain, K.-K. Jespersen, J. D. Westbrook, and G. R. Bird, *J. Phys. Chem.*, **96**, 7988 (1992) and references therein.
14. M. J. S. Dewar and W. Thiel, *J. Am. Chem. Soc.*, **99**, 4899 (1977).
15. M. J. S. Dewar, E. G. Zoebisch, E. F. Healy, and J. J. P. Stewart, *J. Am. Chem. Soc.*, **107**, 3902 (1985).
16. J. J. P. Stewart, *J. Comput. Chem.*, **10**, 209 (1989).
17. G. Rauhut, J. Chandrasekhar, and T. Clark, Oxford Molecular Ltd., Oxford, 1993, implemented on PCs by B. Wiedel.
18. *MOPAC, Version 4.0*, QCPE, program 455, Department of Chemistry, Indiana University, Bloomington, IN.
19. *AMPAC, Version 1.0*, QCPE, program 506, M. J. S. Dewar Research Group.
20. D. B. Boyd, D. W. Smith, J. J. P. Stewart, and E. Wimmer, *J. Comput. Chem.*, **9**, 387 (1988).
21. G. Rauhut, T. Clark, and T. Steinke, *J. Am. Chem. Soc.*, **115**, 9174 (1993).
22. (a) H. Nakano, T. Tsuneda, T. Hashimoto, and K. Hirao, *J. Chem. Phys.*, **104**, 2312 (1996); (b) T. Hashimoto, H. Nakano, and K. Hirao, *J. Chem. Phys.*, **104**, 6244 (1996).
23. T. Koopmans, *Physica* (*Utrecht*), **1**, 104 (1933).
24. L. Radom, W. J. Hehre, and J. A. Pople, *J. Am. Chem. Soc.*, **94**, 2371 (1972).
25. S. Mizushima, *Structure of Molecules and Internal Rotation*, Academic Press, New York, 1954.
26. E. M. Ebeid and S. H. Kandil, *J. Photochem.*, **32**, 387 (1986).
27. A. Gilbert, and J. Baggott, *Essentials of Molecular Photochemistry* Blackwell, London, 1991.
28. J. J. P. Stewart, In *Semiempirical Molecular Orbital Methods*, K. B. Lipkowitz and D. B. Boyed, Eds., VCH, New York, 1990, p. 70.
29. H. Nakanishi, W. Jones, J. M. Thomas, M. Hasegawa, and W. L. Rees, *Proc. R. Soc. London A*, **369**, 307 (1980).